

Estimation of fundamental period of reinforced concrete shear wall buildings using self organization feature map

Mehdi Nikoo^{1a}, Marijana Hadzima-Nyarko^{*2}, Faezehossadat Khademi^{3b} and Sassan Mohasseb^{4c}

¹Young Researchers and Elite Club, Ahvaz Branch, Islamic Azad University, Ahvaz, Iran

²Faculty of Civil Engineering, University of J.J. Strossmayer, 31000 Osijek, Vladimira Preloga 3, Croatia

³Civil and Environmental Engineering Department, Illinois Institute of Technology, Chicago, USA

⁴Technical Director Smtreeam GmbH, 8706 Meilen, Switzerland

(Received August 22, 2016, Revised May 13, 2017, Accepted May 15, 2017)

Abstract. The Self-Organization Feature Map as an unsupervised network is very widely used these days in engineering science. The applied network in this paper is the Self Organization Feature Map with constant weights which includes Kohonen Network. In this research, Reinforced Concrete Shear Wall buildings with different stories and heights are analyzed and a database consisting of measured fundamental periods and characteristics of 78 RC SW buildings is created. The input parameters of these buildings include number of stories, height, length, width, whereas the output parameter is the fundamental period. In addition, using Genetic Algorithm, the structure of the Self-Organization Feature Map algorithm is optimized with respect to the numbers of layers, numbers of nodes in hidden layers, type of transfer function and learning. Evaluation of the SOFM model was performed by comparing the obtained values to the measured values and values calculated by expressions given in building codes. Results show that the Self-Organization Feature Map, which is optimized by using Genetic Algorithm, has a higher capacity, flexibility and accuracy in predicting the fundamental period.

Keywords: fundamental period; Reinforced Concrete Shear Wall (RC SW) buildings; Genetic Algorithm (GA); nonlinear regression analysis; Self-Organization Feature Map (SOFM)

1. Introduction

The elastic demand of reinforced concrete (RC) structure and, indirectly, the required inelastic performance in static procedures is determined by the structure's natural or fundamental period. Hence determining the natural period of a structure is an essential procedure in earthquake design and assessment (Asteris *et al.* 2017). The fundamental period of a structure depends on the mass, stiffness and strength of the structure and is thus affected by many factors, which include structure regularity the height of the building, the provision of shear walls, the number of storeys, number of spans, dimensions of the member sections, presence of openings in the infill panels, position of load, soil flexibility etc. (Asteris *et al.* 2015).

Shear walls (SW) are commonly put into multi-storey buildings due to their good performance under lateral loads, such as earthquake forces, because they provide lateral stability and act as vertical cantilevers in resisting

horizontal forces. Stiffness, strength and ductility are the basic criteria that the structure should satisfy and shear walls provide a nearly optimum means of achieving these objectives (Ahmadi and Bakar 2014, Massone and Ulloa 2014). Buildings having SW are stiffer than framed structures resulting in reduced deformations under earthquake load. Compared to stiffer constructions, flexible buildings that have a greater value of the fundamental period (Işık and Kutanis 2015) experience minor inertial force caused by an earthquake, but will, however, suffer more strain.

According to Poovarodom (2004), there are three main methods of determining the dynamic properties of buildings: using empirical formula, numerical calculation using a model and finally, measurement of the actual system. The empirical formula in codes, currently available for the fundamental period, is a simple relation between the periods of buildings and their geometry. It is worth mentioning that in the vibration modes assessment phase of a specific structure, a large amount of the seismic energy is absorbed using the fundamental mode. For this reason, empirical formulas have been provided by many scientists using many approaches which take into account both the mechanical and geometrical characteristics of the structure. This approach is considered as a rough estimation, but the predictions made by using only a few of building configuration data were shown to be as accurate as more complex computer based methods (Ellis 1980).

The most reliable estimates of periods are from structures which have experienced strong earthquakes and

*Corresponding author, Associate Professor

E-mail: mhadzima@gfos.hr

^aM. Sc. Degree

E-mail: sazeh84@yahoo.com

^bPh.D.

E-mail: fkhademi@hawk.iit.edu

^cPh.D.

E-mail: smteam@gmx.ch

been shaken strongly but not deformed into the inelastic range. However, this is often difficult to achieve since such data of periods are slow to accumulate. There are three reasons for this: first, relatively few buildings are installed with accelerographs, and second, earthquakes causing strong motions of these instrumented buildings are infrequent (Goel and Chopra 1998). The third reason is that this database is further reduced by analyzing distinguishing materials (steel, concrete etc.), structural systems (RC frames, SW etc.) and amplitude of shaking (Michel *et al.* 2010).

An overview of previous research considering experimental monitorization of real buildings is given in section 2. From the available data published from scientists, a database of RC SW buildings, along with the periods measured in both directions is created.

In order to obtain a realistic estimation of seismic demand, many authors propose to evaluate the vibration period based on empirical data from existing buildings subjected to earthquakes. It is pointed in Ricci *et al.* (2011) that seismic codes often adopt formulas obtained by using this procedure. In the following, empirical-based expressions for evaluating the period of vibration of RC SW buildings are illustrated.

In order to characterize the real structure's responses to strong earthquake motion, finite element models of the test structure in dynamic analysis are used and can be verified by performing full-scale ambient and forced vibration experiments (Kutanis *et al.* 2016). Recently, many studies have been published where inappropriate behavior of structures under dynamic loads have been shown. Since the mathematical models of dynamic structural systems based on measured data also have a significant potential for ambient vibration, Zhou *et al.* (2017) pointed out the differences between experimental dynamic analysis tests and refined numerical modeling. Also, many researchers have shown that code formulas are grossly inadequate when comparing with conducted full-scale on-site vibration tests (Lee *et al.* 2000, Gilles *et al.* 2010, Zhou *et al.* 2017).

The aim of this paper is to develop a method to provide a good estimate of the fundamental period of RC SW buildings for the purpose of using it in equivalent lateral force analysis specified in building standards. Since the fundamental period of vibration calculated by currently available approximate equations show remarkable differences between "code-estimated" and "measured" period values for actual structures, one of the contributions of this paper is to create a database of measured periods of real RC SW buildings. This database of RC SW buildings consists of known parameters such as numbers of stories, height, length, width, the percentage of RC walls along with measured vibration periods. In earthquake resistant designs, the value of the fundamental period needs to be as accurate as possible; therefore, using the database of real measurements, another contribution of the paper is to use new methods, such as ANN to provide more accurate prediction of fundamental periods. The Self-Organization Feature Map (SOFM) is used for modelling the expressions for fundamental period and then Genetic Algorithm (GA) is used in optimizing the SOFM models. The results between

the best SOFM Model and values obtained by code are presented and discussed in this paper.

2. Previous researches of dynamic characteristics of reinforced buildings by experimental monitorization

Essentially, according to Oliveira and Navarro (2010), there are two ways to obtain the dynamic characteristics of a building: 1) by experimental monitorization of a real building for different input motion; 2) by numerical modelling based on the mechanical properties of building components. Both are important and complementary, with the second one being a way to calibrate the first.

Housner and Brady (1963) published a theoretical analysis for an idealized building with shear walls with expressions derived using the Rayleigh's method.

Cole *et al.* (1992) compared expressions for periods given in UBC-91 with the data recorded on 64 buildings during some Californian earthquakes.

Measurements from 21 buildings during the Loma Prieta and Whittier earthquake were analyzed in the work of Li and Mau (1997). The measured fundamental periods were compared with the expressions from UBC-94 code. It was noticed that the fundamental period of RC frames were underestimated, while the period of SW buildings were overestimated in some cases and underestimated in other cases.

In the work of Goel and Chopra (1998), fundamental periods of SW buildings were measured on 16 buildings during several Californian earthquakes and compared with the values given by codes. It was discovered that the expressions in codes resulted in a longer fundamental period than the measured one which produced non-conservative shear forces. When different values of C_i (Eq. (1)) derived from the combined effective area were used, the result was a much shorter period than the measured one. It was also concluded that the expression from ATC3-06, which used building dimension as the base for the investigated direction, significantly underestimated the period. Goel and Chopra also proposed new expressions based on Dunkerley's method and the restriction of the period to 1.4 times the value from rational analysis.

Lee *et al.* (2000) measured fundamental periods on 50 RC apartment buildings with shear walls, and these results were compared with those obtained by code formulas and also by dynamic analysis. The comparison showed that comparatively large errors were likely to occur when code formulas were used.

In the work of Jalali and Salem (2005), ambient vibration measurements were conducted on 30 RC buildings in Tehran and Tabriz, designed according to Iranian code, and the results of those measurements were compared to code formulas.

Likewise, Gallipoli *et al.* (2010) performed ambient noise measurements on 244 RC buildings from 1 to 20 floors in four European countries. It was found that the most striking feature was the similarity of the height-period relationships in four countries.

In the work of Kwon and Kim (2010), building period

Table 1 Expressions for periods of RC SW buildings given in building codes and by researchers

Building Code	Formula	Eq.	Units
FEMA-450 (2003)	$T = C_t \cdot H^{0.75}; C_t = 0.0488$	(3)	(meters; square meters)
ATC3-06 (1978)	$T = \frac{0.05H}{\sqrt{D}}$	(4)	(feet)
Korean Code (1998)			
Indian Seismic Code (IS IC-413) (2002)	$T = \frac{0.09H}{\sqrt{D}}$	(5)	(meters)
Egyptian Code (1988)			
Costa Rican code (1986)	$T = 0.05N$	(6)	-
UBC-97 (1997) and SEAOC96 (1996)	$T = C_t \cdot H^{0.75}; C_t = \frac{0.1}{\sqrt{A_c}}; A_c = \sum_{i=1}^{NW} A_i \left[0.2 + \left(\frac{D_i}{H} \right)^2 \right]; \frac{D_i}{H} \leq 0.9$	(7)	(feet; square feet)
EC8 (2004)	$T = C_t \cdot H^{0.75}; C_t = \frac{0.075}{\sqrt{A_c}}; A_c = \sum_{i=1}^{NW} A_i \left[0.2 + \left(\frac{D_i}{H} \right)^2 \right]; \frac{D_i}{H} \leq 0.9$	(8)	(meters; square meters)
EAK (2003)			
Greek Seismic Code	$T = 0.09 \cdot \frac{H}{L} \sqrt{\frac{H}{H + \rho L}}$	(9)	(meters)
NSCP (1992)			
Philippine Code	$T = C_t \cdot H^{0.75}; C_t = \frac{0.03048}{\sqrt{A_c}}; A_c = \sum A_i \left[0.2 + \left(\frac{D_i}{H} \right)^2 \right]$	(10)	(meters; square meters)
NZSEE (2006)			
New Zealand Seismic Code	$T = 1.25 \cdot k_t \cdot H^{0.75}; k_t = \frac{0.75}{\sqrt{A_c}}; A_c = \sum \left[A_i \left(0.2 + \frac{D_i}{H} \right)^2 \right]; \frac{D_i}{H} \leq 0.9$	(11)	(meters; square meters)
Goel and Chopra (1998)	$T_L = 0.0019 \frac{1}{\sqrt{A_e}} H; A_e = \sum_{i=1}^{NW} \left(\frac{H}{H_i} \right)^2 \left[\frac{A_i}{1 + 0.83 \left(\frac{H_i}{D_i} \right)^2} \right]; \bar{A}_e = 100 \frac{A_e}{A_B}$	(12)	(feet; square feet)
Goel and Chopra (1998)	$T_U = 0.0026 \frac{1}{\sqrt{A_e}} H; A_e = \sum_{i=1}^{NW} \left(\frac{H}{H_i} \right)^2 \left[\frac{A_i}{1 + 0.83 \left(\frac{H_i}{D_i} \right)^2} \right]; \bar{A}_e = 100 \frac{A_e}{A_B}$	(13)	(feet; square feet)

formulas in seismic design code with over 800 apparent building periods from 191 building stations and 67 earthquake events were evaluated. The evaluation was carried out with the formulas in ASCE 7-05 for steel and RC MRF, SW buildings, braced frames and other structural types. The differences between the periods from code formula and measured periods of low-to-medium rise buildings were relatively high. The code formula for SW buildings overestimated periods for all building heights.

3. Existing formulas of RC SW buildings

Among the critical load cases accounted for in design of new buildings or evaluation of existing ones are seismic loadings (Ozmen and Inel 2015). In the earthquake resistant design of a structure, the forces that act on the structure must be determined. However, the actual forces that will occur over the lifetime of the structure cannot be known. Seismic forces to the structure result from the vibration of mass of structure. The fundamental period appears in the equations given in the standards or codes for the calculation of yield base shear and lateral forces. Therefore, during the building planning and design phases, it is important to

carefully consider the fundamental period of the building.

In the majority of cases, the assessment of the period is considered as a function of the structural system classification and number of stories or height and/or wall area. Several different expressions for evaluating the vibration period of RC SW buildings are given further in the text. A brief overview of the design equations provided in various codes and standards to estimate the fundamental natural period can be found in a work of Sofi *et al.* (2015).

The formulation of period-height relationships is typically of the type

$$T = \alpha \cdot H^\beta \quad (1)$$

where H represents the height of the system and α and β are constants. Since it first appeared in U.S. building code ATC3-06 with β equal to 0.75, the first empirical formula was in the following form

$$T = C_t \cdot H^{0.75} \quad (2)$$

where: H – height of the structure [m] and C_t – constant depending on the structure type.

The coefficient C_t is calibrated in order to achieve the best fit to experimental data. The value of C_t is given in

Table 1.

This particular form of Eq. (1) was theoretically derived using Rayleigh's method with the assumptions that the equivalent static lateral forces are distributed linearly over the height of the structure, the seismic base shear is proportional to $1/T^{2/3}$ and the distribution of the stiffness with height produces a uniform inter-story drift under the linearly distributed horizontal forces.

Empirical expressions given in building codes are presented in Table 1 where:

A_c – the total effective area of the shear walls in the first storey of the building (m^2),

A_i – the effective cross-sectional area of shear wall „ i ” in the direction considered in the first storey of the building (m^2),

D_i – length of the shear wall „ i ” in the first storey in the direction parallel to the applied load (m), with the restriction $D_i/H \leq 0.9$;

A_e – equivalent shear area assuming that the stiffness properties of each wall are uniform over its height;

\bar{A}_e – the equivalent shear area expressed as a percentage of A_B , which represents the building area;

L – the width of structure in the direction of analysis (in meters);

ρ – the ratio of the areas of shear wall sections along the direction of analysis to the total area of walls and columns.

N – total number of stories.

4. Selected buildings and identification of fundamental periods

A database containing 78 building periods is created in order to evaluate the approximate period formulas in current seismic codes, provided in the previous section. Among various lateral load-resisting systems and their measured periods published in literature, only buildings with RC shear walls were selected. After reviewing the plans of the buildings, buildings with large irregularity, base isolation systems, or energy dissipation systems were excluded. In order for an RC SW building to be selected into the database, all the following parameters have to be known:

- plan dimensions;
- percentage of RC walls in both directions, e.g. RC wall area in both directions;
- number of storey;
- storey height.

The majority of the buildings in the database were taken from the data provided by Lee *et al.* (2000). They carried out full-scale measurements on 50 RC apartment buildings in order to evaluate the reliability of code formulas such as those of the current Korean Building Code (KBC), UBC 1997, NBCC 1995 and BSLJ 1994 for estimating the fundamental period of RC SW buildings. The results of measured periods were compared with those obtained by code formulas and those by dynamic analysis. Large errors occurred when the code formula of KBC, which is based on UBC 1988, was used. Also, none of the other code formulas examined in the study were sufficient for estimating the fundamental period of apartment buildings with SW

dominant systems. The measured 10 to 25 storey high buildings were RC structures consisting of walls and regularly shaped flat plate slabs without columns or beams, and a centrally located rectangular core or cores spaced by two housing units. The thickness of walls and slabs of these buildings with various sizes and plan shapes were almost equal (about 200 mm), and the walls in units and cores, which were the primary lateral force resisting elements, were continuous throughout the height of such buildings. The storey height was about 2.6 m for all stories. Each building had a mat or a pile foundation. Since all the aforementioned parameters of all buildings were known, all 50 buildings were included in the database. Their height varied from 40 to 68 m (or 15 to 25 stories) and had different plan dimensions. The ratio of the shear wall area aligned in the direction of the periods compared to the plan area of a typical floor varied from 1.4 to 6%. The length of the buildings varied from 18.3 to 63.9 m, while the width varied from 10 to 12.83 m.

Gilles (2010) started to develop a period database for the city of Montreal, Canada, using ambient vibration measurements and the Frequency Domain Decomposition method. Between June 2007 and August 2009, ambient vibration tests were performed in 39 buildings in Montréal, from which 27 RCSW provided the main resistance to lateral loads. The database represented a consistent data set for the low-amplitude fundamental periods of buildings in Montreal, which have been used to evaluate the NBCC 2005 formulas, to develop improved period equations and could have been used for seismic vulnerability studies in Montreal and as a pre-damage benchmark for the measured buildings (Gilles, 2008). Only 17 of the 27 RC SW buildings were selected for our database due to the constraints mentioned at the beginning of the section. The number of stories varied from 6 to 49, i.e., from 23 to 195 m. The ratio of the shear wall area aligned in the direction of the periods compared to the plan area of a typical floor varied from 0.24 to 1.35%.

Nine buildings were selected from the data provided by Goel and Chopra (1997). The authors evaluated the formulas specified in U.S. codes using the available data on the fundamental period of buildings, “measured” from their motions recorded during eight California earthquakes. The height of the buildings included in the database ranged from 3 to 10 stories and the ratio of the shear wall area aligned in the direction of the periods compared to the plan area of a typical floor varied from 0.29 to 2.45%. The image of one of the measured buildings is presented in Fig. 1(a).

The remaining 2 buildings were taken from the work of Gonzales and Lopez-Almansa (2011). The research was focused on buildings located in Peru with thin walls that were mainly 10 cm thick and reinforcement consisting mainly of a single layer of welded wire mesh. A typical building, which was analyzed, is presented in Fig. 1(b). These buildings might be vulnerable to earthquakes because of their low ductility, which was numerically evaluated by push-over and nonlinear time history analyses and the structural parameters were obtained from available testing information on two buildings with five stories, which were part of this database. Both buildings had a height of 12.1 m



(a) Burbank 10-Story Residential Building, CSMIP Station No. 24385 – investigated by Goel and Chopra (1997) (b) Building investigated by Gonzales and Lopez-Almansa (2011)

Fig. 1 Images of some of the buildings in the database

Table 2 Overview of the database of measured vibration periods for RC SW buildings

Source	No. of buildings selected	No. of storeys		Height (m)		Length (m)		Width (m)		SW area (% with respect to plan area)	
		min	max	min	max	min	max	min	max	min	max
Lee <i>et al.</i> (2000)	50	15	25	40.00	68.00	18.30	63.90	10.00	12.38	1.40	6.00
Gilles (2010)	17	6	49	20.00	195.0	23.00	89.00	20.00	72.00	0.24	1.35
Goel and Chopra (1997)	9	3	10	10.97	45.63	22.86	69.19	18.29	65.63	0.29	2.45
Gonzales and Lopez-Almansa (2011)	2	5	5	12.10	12.10	16.60	28.00	12.10	15.1	2.39	2.96

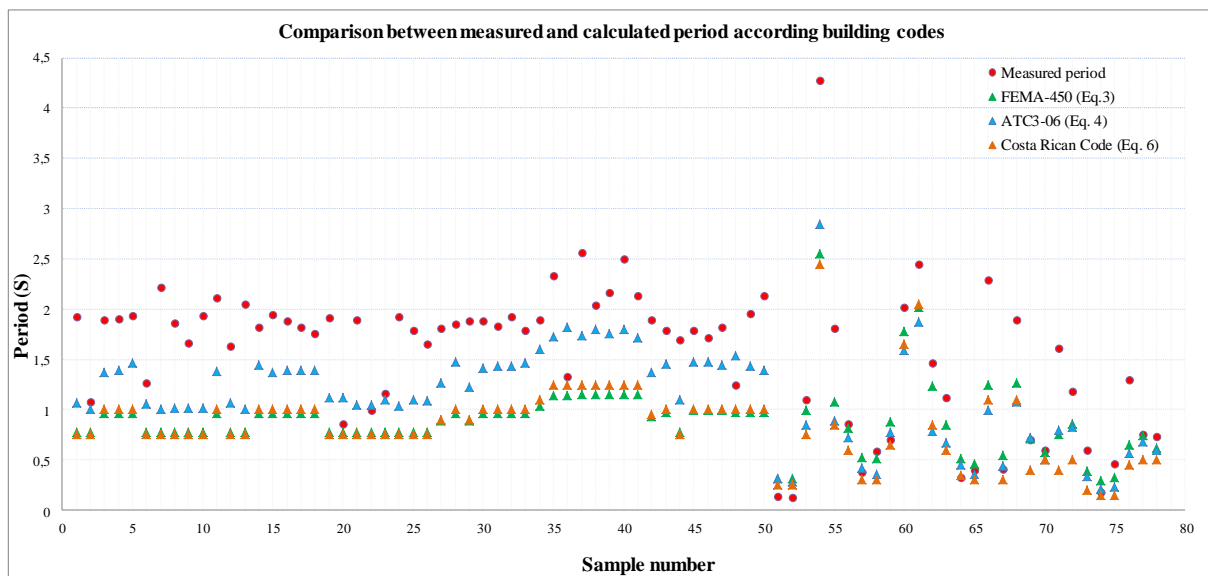


Fig. 2 Comparison between measured and calculated period according to building codes

and sum of the lengths of walls aligned in the direction of the periods compared to the plan area of a typical floor were 2.39% and 2.96%.

An overview of the generated database is given in Table 2.

5. Comparison of measured periods with periods obtained using building codes

In order to evaluate the reliability of period formulas obtained by building codes, the measured periods were compared with those obtained from some of the code

formulas. For all the buildings in the database, the fundamental periods were calculated using only Eqs. (3), (4) and (6). Eq. (5) is similar to Eq. (4) when feet are converted into meters. The fundamental periods were not calculated using the other Equations, i.e., (7) to (13) since the extra data they require (width and length of the RC walls) were not available for all the buildings. Therefore, in Fig. 2, the comparison between the measured and calculated periods according to FEMA-450 (Eq. (3)), ATC3-06 (Eq. (4)) and Costa Rican Code (Eq. (6)) is presented. It is observed that for a majority of the buildings, the formulas (Eqs. (3), (4) and (6)) give a period much shorter than the

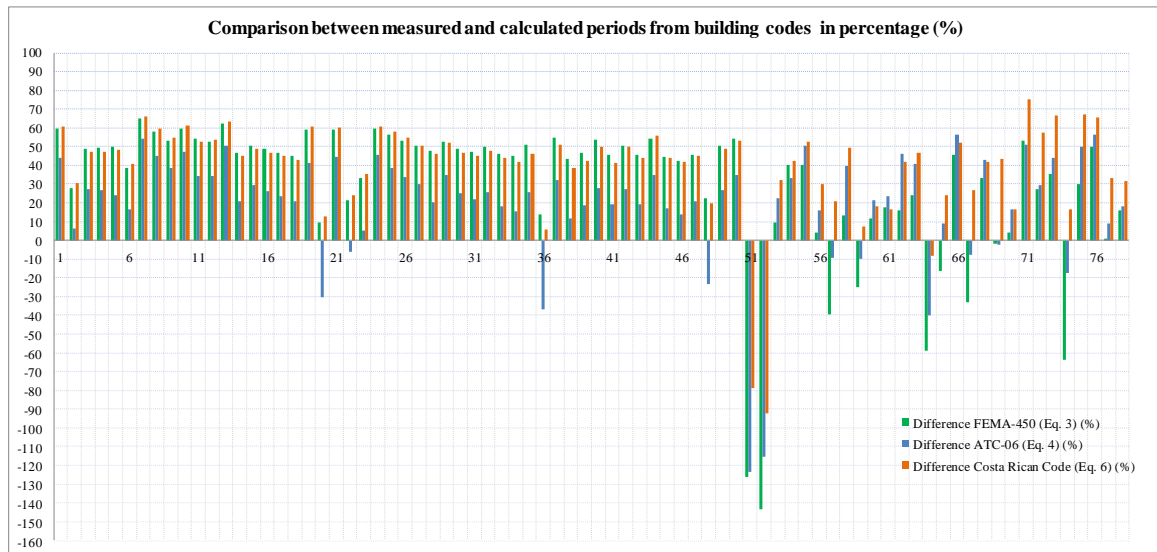


Fig. 3 Comparison in percentages between measured and calculated period according to building codes

one measured in this study.

Fig. 3 shows the percentage difference between the measured and calculated fundamental periods. It can be seen that for most buildings, the differences are generally between 30% and 60%. In couple of cases, the percentage errors are much higher. The percentage differences between the measured and calculated period according to ATC3-06 (Eq. (4)) were slightly lower, but for most buildings the differences were greater than 30%. Generally, it can be seen from Figs. 2 and 3 that among the three formulas given in seismic codes, the smallest errors are obtained using the formula ATC3-06 (Eq. (4)).

Building periods predicted by these empirical equations are widely used in practice although it has been pointed out by many (Goel and Chopra 1998, Lee *et al.* 2000, Hadzima-Nyarko *et al.* 2015, Salama 2015) that there is room for further improvement in these equations.

The comparison of the measured values with empirical values indicates the potential of using ANNs for the prediction of the fundamental period of RC SW structures taking into account the crucial parameters that influence its value.

In the last decades, there have been many attempts to use artificial neural networks in structural engineering (Hadzima-Nyarko *et al.* 2011, Kalman Šipoš *et al.* 2013, Lazarovska *et al.* 2014, Aguilar *et al.* 2016); however, to the authors' best knowledge, there have been only a few attempts to apply ANNs for the prediction of the fundamental period of framed and infilled framed structures (Kose 2009, Joshi *et al.* 2014, Asteris *et al.* 2016) and no attempt for the prediction of the fundamental period of RC SW buildings.

6. Defining the Self-Organization Feature Map (SOFM) and Genetic Algorithm (GA)

Data-driven models are used extensively by different scientists. Khademi *et al.* (2015) used ANN model for

predicting the compressive strength of concrete. Nikoo *et al.* (2015) estimated the concrete compressive strength using evolutionary ANN. Muhammad *et al.* (2016) used a number of 3-layer Back propagation Neural Network (BPNN) as well as sensitivity analysis in shotcrete mix design modeling. In the current study, SOFM and GA are used as predictor models which are explained comprehensively in the following.

6.1 Self-Organization Feature Map and Kohonen network

In SOFM, competitive learning is used for training and it is improved using specific features of the human brain. The cells in human brain are presented with regular and significant computational maps in different sensory areas of the brain (Kohonen 1989). In a SOFM system, processing units are located in the nodes of one, two or more dimensional networks. Units are arranged in the competitive learning process with respect to input patterns. The location of the arranged units in the network should lead to the creation of a meaningful coordinate system in the network for input characteristics (Kohonen 1989). Hence, a SOFM contains a topographic map of input patterns in which the location of units corresponds to the inherent properties of the input patterns. Competitive learning, which is most of the times used in these types of networks, means that in each learning step units compete with each other in order to be activated. In the final step of each competition, just one unit wins, that is, its weights are changed differently in comparison to other units. In other words, when a new learning sample is applied to the network, the Euclidean distance from the weight vector of all the neurons in the network is calculated. The neuron with weight vector most similar to the input vector will be the winner. This learning is called Unsupervised Learning. Self-Organization Feature Maps are divided into different groups based on their structure; (1) MaxNet Network, (2) Mexican Hat Network, (3) Hamming Network, and (4) Kohonen Network.

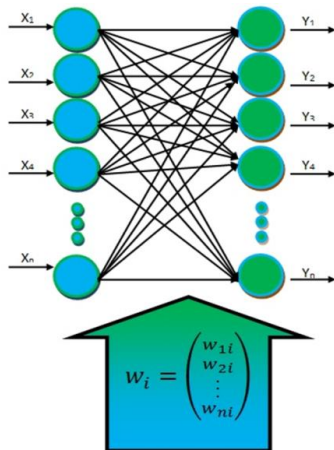


Fig. 4 Model of one dimensional Kohonen Network (Srinivas *et al.* 2005)

Kohonen is different from other neural networks due to its maintenance of the spatial characteristics of the input space. The reason for using Kohonen network is the increase of distinction among the inputs. In this network, each unit with positive weights is connected to its partner neighbors and each unit with negative weights is connected to its rival neighbors. Weight attributions represent the fact that the weights have positive values in the neighborhood of the partners and negative values in the neighborhood of the rivals. In the late 70's, Kohonen showed the important fact that the reason of learning rule should be construction of the w_i vectors collection, which points out the equal reliability representation of one density function with the constant reliability of ρ . In other words, w_i vectors should change themselves based on the fact that each x input vector and density function with the constant reliability of ρ (14) (Kohonen 1989)

$$\rho(X) = \frac{1}{m} \quad (14)$$

One Kohonen layer is an array of neurons that can be one, two, or more dimensional. Examples of this type of network are shown in Figs. 4 and 5.

In the learning phase of each unit, the distance of the X input vector to its own weights is calculated using Eq. (15) (Kohonen 1989)

$$li = D(X, w_i), \quad (15)$$

in which D is the distance measuring function. It is worth mentioning that any distance measuring function can be used for this purpose, for example Eq. (16) (Kohonen 1989)

$$D(u, v) = 1 - \cos\theta. \quad (16)$$

In order to calculate the angle between $\theta = v, u$ the Euclidean distance formula $D(u, v) = |u - v|$ can be used. The reason for this is to find out whether the units have the nearest weight vectors to X or not. This part is explained as the competitive part in these types of networks. The units with the closest weight to the input layer would be declared as the winner of this competition where its z_i value would be equal to one. It is worth mentioning that in this situation,

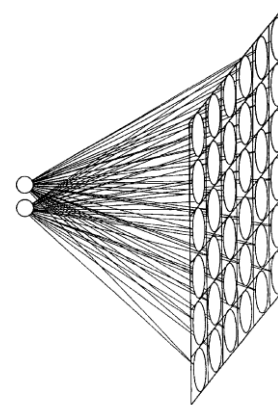


Fig. 5 Model of two dimensional Kohonen Network (Nikoo *et al.* 2015)

the z_i of other units would be equal to zero. Finally, the Kohonen Rule which is shown in Eq. (17) can be used for the purpose of updating the weights (Kohonen 1989)

$$w_i^{new} = w_i^{old} + \alpha (X - w_i^{old}) z_i \quad 0 < \alpha \leq 1 \quad (17)$$

Eq. (17) can be also presented as Eq. (18), which is shown as follows (Kohonen 1989)

$$w_i^{new} = \begin{cases} (1 - \alpha)w_i^{old} + \alpha X & \text{for winner} \\ w_i^{old} & \text{other unites} \end{cases} \quad (18)$$

SOFM, which is an unsupervised learning algorithm, has been proposed by Kohonen in 1982 for the first time (Kohonen 1989). The output neurons in this method are generally in a form of rectangular or hexagonal lattice which are organized into a one or two-dimensional map. It should be noted that in this method each of the output neurons is connected to all input neurons (Tay *et al.* 2001).

The competitive learning algorithm is implemented in SOFM. For a specified input, the neuron that corresponds best to the situation, wins the competition and is permitted to be updated towards the input vector. Both the neurons and neighbors are allowed to be updated in SOFM (Tay *et al.* 2001).

6.2 Genetic algorithm optimization method

GA gets its inspiration from nature. It can be defined as evolutionary optimization algorithms based on Darwin's principle of "Survival of the fittest". It employs computational models of evolutionary processes such as selection, crossover and mutation as stochastic search techniques for finding global minimum for complex non-linear problems having numerous sub-optimal solutions. GA is able to offer a delightful blend of exploration and exploitation of the search space. The GA parallel nature of global search and gradient free optimization and utilization of stochastic operators help in evolving the initial weights for ANN, thereby minimizing the likelihood of the BP algorithm to get stuck in the local minima (Chandwani *et al.* 2015).

In the system of genetic algorithm, genetic information is stored in chromosomes. Chromosomes are replicated and

Table 3 Statistical characteristics of the database data

No.	Parameter Name	Type	max	min	mean	STDEV
1	No. of storeys	Type	49	3	16.81	7.702
2	Height	Input	195	10.97	49.92	26.42
3	Length	Input	89	16.6	42.34	13.49
4	Width	Input	72	10	18.79	12.81
5	Longitudinal SW area	Input	27.4615	0	12.13	5.33
6	Transverse SW area	Input	41.34742698	2.672	18.64	8.864
7	Fundamental period	Output	4.273504	0.13	1.555	0.698

passed onto the next generation with selection depending on fitness. Genetic information can also be altered through genetic operations such as mutation and crossover. In GA, each “chromosome” is a set of genes, which constitutes a candidate solution of the problem. In typical implementations, a population or subpopulations of “chromosomes” are used. The passage of each “chromosome” to the next generation is determined by its relative fitness. Random mixtures and/or changes of the transmitted “chromosomes” produce variations in the next generation of “offspring”. The individuals that have greater fitness values (correspondence with desired properties) have better chances of being selected for transmission (Yuan *et al.* 2014). GA is hybridized with ANN in order to improve the performance of ANN and to reduce the drawback of BP algorithm. This procedure involves two stages. In the first stage, ANN is trained using GA. GA is used for evolving the optimal set of initial weights and biases for training of the neural network. This is accomplished by simultaneous search performed by GA in all possible directions in the search space and narrowing down to the region where there is maximum probability of finding the optimal weights and biases. The second stage involves training of neural network using BP algorithm. The training is started by initializing the BP algorithm with set of initial weights and biases evolved using GA assisted training of ANN. This initialization of ANN with optimal weights and biases is harnessed by BP algorithm to carry forward the search for

the global optima started by GA through fine tuning of neural network’s weights and biases. In this method, higher qualified chromosomes have more chance for being repeated on selected population.

7. Research process

In this section, an overview of the research process regarding the data and methodology is provided.

7.1 Defining the study data

According to the data explained in section 4, a database of 78 RC SW buildings was created. The overall statistical characteristics of the created database of fundamental periods of RC SW buildings are given in Table 3.

7.2 Methodology

The number of inputs and outputs in the SOFM is six and one, respectively. In this research, three different Kohonen networks which are Square, Line, and Diamond are used for training. The overall specimens are 78 in which 80 percent of them (62 specimens) are used for training purposes and 10 percent of them (8 specimens) are used for cross validation and another 10 percent of them (8 specimens) are used for testing. Different excitation functions of Linear Axon, Bias Axon, Linear Sigmoid Axon, Linear Tanh Axon, Sigmoid Axon, Tanh Axon were used in order to determine the structure of the SOFM. For the purpose of determining the number of hidden layers, the experimental formula (19) was used in addition to default software (Gavin and Bowden 2005)

$$N_H \leq 2N_I + 1 \tag{19}$$

where N_H is the maximum number of the hidden layers and N_I is the number of inputs. Based on the fact that the number of effective inputs is equal to 6, the maximum number of nodes of hidden layers would be equal to 13 ($N_H \leq 13$). The NeuroSolutions software (NeuroSolutions 2005) is used in determining the optimized structure of each

Table 4 Optimized model of Self-Organization Feature Map using Genetic Algorithm

Row	Model Name	No. of Inputs	No. of Outputs	No. of Hidden Layers	Learning Rule	No. of Nodes in the Hidden Layer	Network SOFM (Rows and Columns)	Transfer Function	Neighbourhood Shape	Characteristics of Genetic Algorithm
1	<u>Model 1</u>			<u>1</u>	<u>Moment</u>	<u>6</u>	<u>5*5</u>	<u>Tanh Axon</u>	<u>SquareKohonenfull</u>	Crossover One point
2	Model 2			2	Step	8_4	6*6	<u>Linear Tanh Axon</u>	LineKohonenfull	Crossover probability 0.9
3	Model 3			3	Delta Bar Delta	4_4_4	7*7	<u>Linear Axon</u>	DiamondKohonenfull	
4	Model 4	<u>6</u>	<u>1</u>	1	QuickProp	13	6*6	<u>Linear Axon</u>	<u>SquareKohonenfull</u>	Mutation probability <u>0.01</u>
5	Model 5			2	<u>Moment</u>	7_6	7*7	<u>LinearTanhAxon</u>	LineKohonenfull	
6	Model 6			2	<u>Moment</u>	4_4	5*5	<u>SigmoidAxon</u>	DiamondKohonenfull	Generation 100

Table 5 Optimized models of Self-Organization Feature Map in train, validation, and test steps for the fundamental period output

Row	Model	Train		Validation with Train		Test	
		Results of Graphs		Results of Graphs		Results of Graphs	
		Equation	R^2	Equation	R^2	Equation	R^2
1	SOFM Model 1	$y=0.8972x+0.2218$	0.9275	$y=0.9243x+0.1098$	0.9442	$y=0.9117x+0.1127$	0.9436
2	SOFM Model 2	$y=0.6357x+0.7184$	0.6815	$y=0.6954x+0.5507$	0.7428	$y=0.8544x+0.2276$	0.85
3	SOFM Model 3	$y=0.4959x+0.9621$	0.8556	$y=0.4959x+0.9621$	0.8556	$y=0.524x+0.7508$	0.5483
4	SOFM Model 4	$y=0.498x+0.8178$	0.7622	$y=0.5543x+0.6991$	0.5649	$y=0.5956x+0.5363$	0.6259
5	SOFM Model 5	$y=0.6872x+0.6016$	0.8664	$y=1.0072x-0.0087$	0.9038	$y=0.8169x+0.2897$	0.8119
6	SOFM Model 6	$y=0.0242x+1.5622$	0.7781	$y=0.013x+1.5808$	0.2803	$y=0.0163x+1.5727$	0.3581

Table 6 Statistical index for different SOFM Models for the fundamental period output

Row	Model	Train				Validation				Test			
		MAE	MSE	RMSE	RMSD	MAE	MSE	RMSE	RMSD	MAE	MSE	RMSE	RMSD
		Mean Absolute Error	Mean Squared Error	Root Mean Squared Error	Mean Root Squared Deviation	Mean Absolute Error	Mean Squared Error	Root Mean Squared Error	Mean Root Squared Deviation	Mean Absolute Error	Mean Squared Error	Root Mean Squared Error	Mean Root Squared Deviation
1	SOFM Model 1	0.022	0.005	0.067	0.402	0.013	0.003	0.053	0.273	0.131	0.029	0.171	0.329
2	SOFM Model 2	0.045	0.022	0.148	0.561	0.028	0.015	0.123	0.369	0.201	0.074	0.273	0.403
3	SOFM Model 3	0.042	0.023	0.153	0.529	0.042	0.023	0.153	0.529	0.310	0.225	0.474	0.488
4	SOFM Model 4	0.038	0.018	0.136	0.496	0.038	0.023	0.150	0.467	0.312	0.198	0.445	0.501
5	SOFM Model 5	0.031	0.012	0.110	0.442	0.018	0.005	0.074	0.329	0.213	0.093	0.305	0.404
6	SOFM Model 5	0.061	0.053	0.231	0.619	0.069	0.054	0.232	0.687	0.537	0.480	0.693	0.683

SOFM. The optimized parameters are the number of hidden layers, number of nodes in hidden layers, learning algorithm of the network, transfer function and optimization ability of genetic function. Table 4 shows the optimized structure of each model and their different characteristics obtained by using GA.

8. Results

The results of training, validation simultaneous with training and testing of each of the models with optimized structures are presented in Table 5. In order to determine the best model, the R^2 criterion and the slope of the straight line of the models are compared. Furthermore, in Table 6, the statistics indexes of all the models are evaluated. As it is shown in Tables 5 and 6, Model 1 has the most correlation for the output data compared to all other models.

Also, the values of the structure in comparison to the corresponding actual measured values are shown in Figs. 6, 7 and 8. As it is shown in Figs. 6, 7 and 8 and Tables 5 and 6, in Model 1 the value of R^2 for the periods of structure during train, validation and test stage is 0.9436, 0.9442 and 0.9275, respectively. In addition, slopes of straight line for this parameter are 0.9117, 0.9243 and 0.8972, respectively.

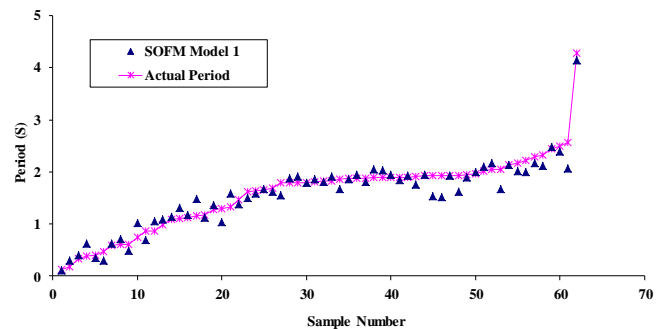


Fig. 6 Comparison of values of fundamental period outputs in SOFM Model with the experimental data in train step

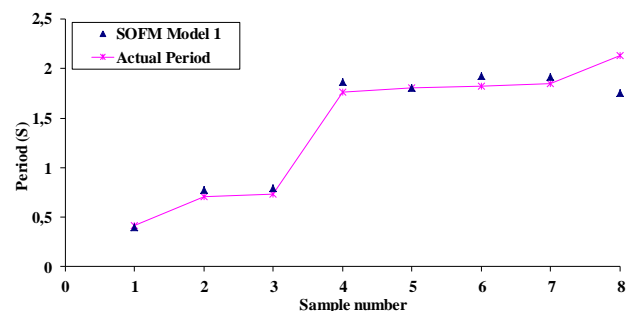


Fig. 7 Comparison of values of fundamental period in SOFM Model in validation step

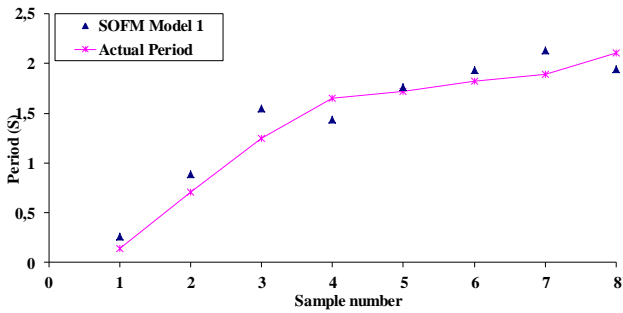


Fig. 8 Comparison of fundamental period output in SOFM model in the test step

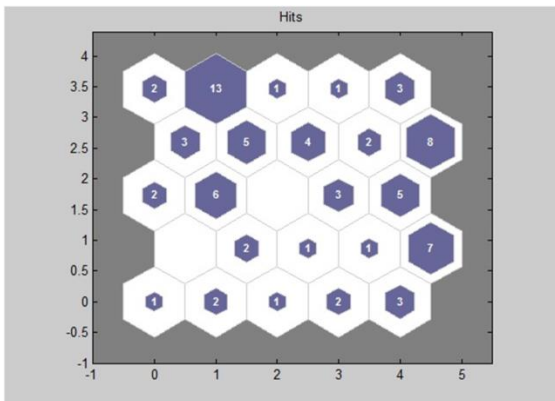


Fig. 9 5*5 Structure for accommodation of input data in SOFM Model 1

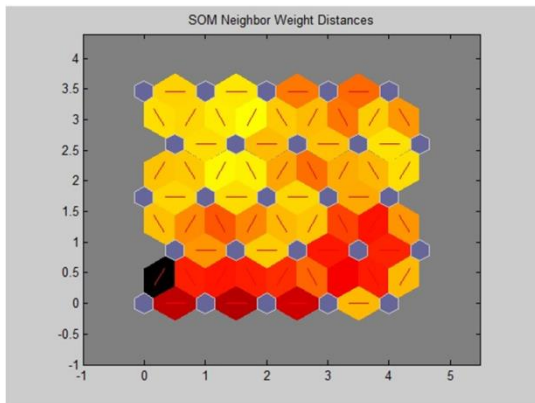


Fig. 10 Effect of distances of neighbourhood weights in 585 structure in SOFM Model 1

Therefore, Model 1 has the highest correlation compared to all other 5 models. It is worth mentioning that SOFM1 has the least value of statistical index which indicates that this model has the least error. The best network for matching the input parameters in SOFM is a 5*5 structure, which is shown in Figs. 9 and 10. This structure indicates the capability of each neuron for absorbing the number of the nodes for the two dimensional structure.

In addition, the greatest impact of input data on the structure of SOFM Model 1 is shown in Fig. 10, which displays the neuron distances based on the lightness and darkness of colours. In other words, the lighter the colour is,

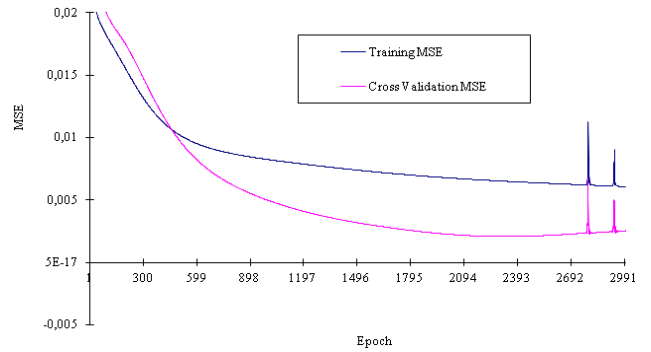


Fig. 11 MSE value per epoch for SOFM Model 1 in both train and cross validation steps

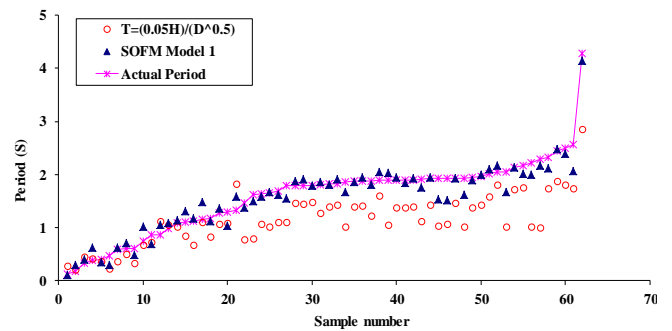


Fig. 12 Comparison of fundamental periods obtained by SOFM Model 1 and ATC3-06 (Eq. (4)) with experimental data in train step

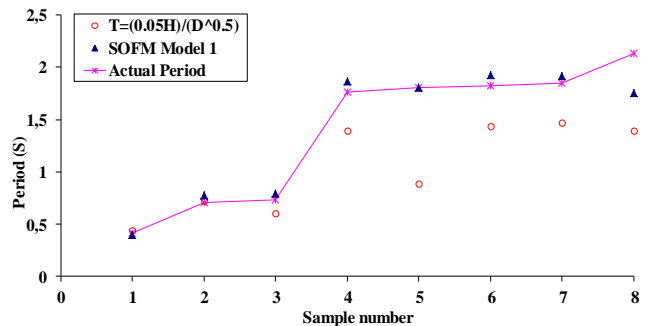


Fig. 13 Comparison of fundamental periods obtained by SOFM Model 1 and ATC3-06 (Eq. (4)) with experimental data in validation step

the less distance the neurons would have. In addition, Fig. 11 represents the convergence rate of MSE in both the train and cross validation steps.

8.1 Comparison of SOFM model with code formula

The best model obtained, SOFM model 1, was compared to the actual values measured and values obtained by building code ATC3-06 code, given by Eq. (4). The results of this comparison are presented in Figs. 12-17. Looking at Figs. 12-14, it can be noticed that the SOFM Model 1 provides a better estimate of the actual values measured compared to the estimate provided by building code ATC3-06. This is further confirmed by analysing Figs. 15-17, where the plot of the predicted values of both the

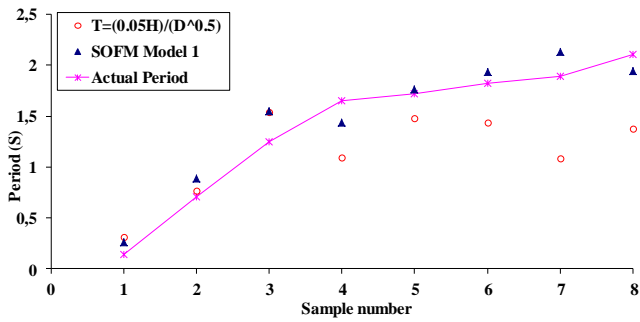


Fig. 14 Comparison of fundamental periods obtained by SOFM Model 1 and ATC3-06 (Eq. (4)) with experimental data in test step

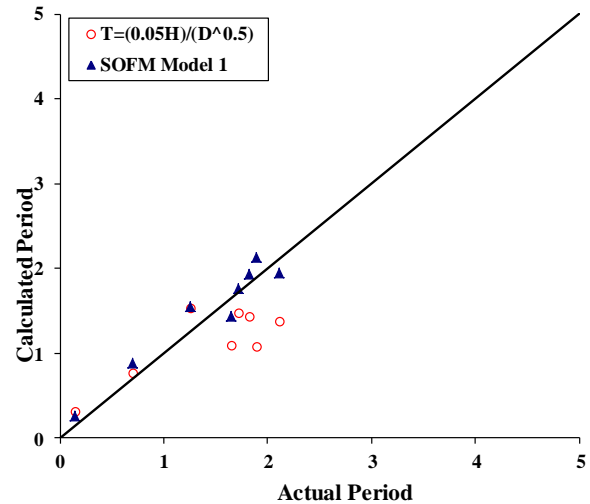


Fig. 17 Comparison of fundamental periods obtained by SOFM Model 1 and ATC3-06 (Eq. (4)) in test step

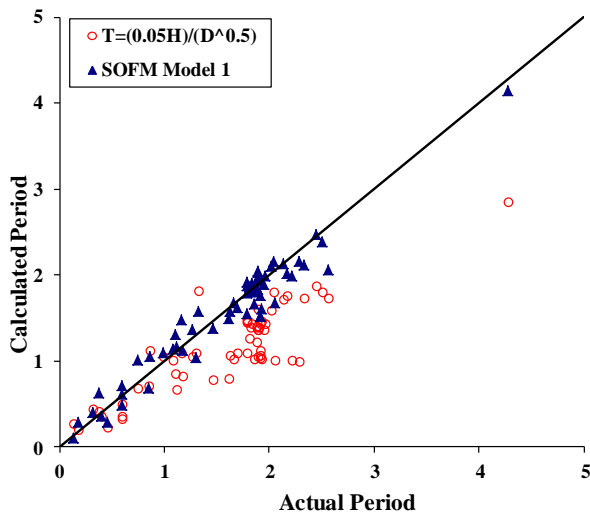


Fig. 15 Comparison of fundamental periods obtained by SOFM Model 1 and ATC3-06 (Eq. (4)) in train step

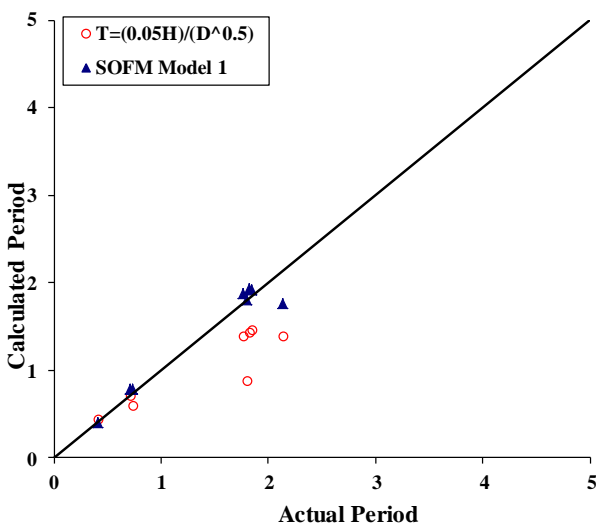


Fig. 16 Comparison of fundamental periods obtained by SOFM Model 1 and ATC3-06 (Eq. (4)) in validation step

SOFM Model 1 and building code ATC3-06 are compared to the actual measurements. The perfect model is depicted by the straight black line $y=x$, hence the closer the model outputs are to the black line, the better the model.

9. Conclusions

The fundamental period of vibration calculated by currently available code expressions show a, in some cases, significant deviation from the measured period values of actual structures. As a result, a lot of research is currently being performed to better these code expressions. This paper presents a step in such a direction. A database of measured periods of real reinforced concrete shear wall buildings is created. Using this database, five different SOFM neural network models are created and weights of the artificial neural networks optimized using genetic algorithm. These models are compared in three different steps: training step, validation simultaneous with training step, and test step. Results show that the SOFM Model 1 with the Square Kohonen full learning algorithm and Tanh Axon transfer function is the best model. This SOFM model was further evaluated by comparing the model outputs to code expression values, taking into consideration the actual period values measured. Results indicate that the SOFM model better predicts fundamental period values compared to code expression values. These preliminary results indicate that practitioners could consider suitably trained neural network models, instead of code expressions for fundamental period estimation. Our future work involves increasing the database and analysing other model structures suitable for period prediction.

References

Aguilar, V., Sandoval, C., Adam, J.M., Garzon-Roca, J. and Valdebenito, G. (2016), "Prediction of the shear strength of reinforced masonry walls using a large experimental database and artificial neural network", *Struct. Infrastruct. Eng.*, **12**(12), 1663-1676.

Ahmadi, M. and Bakar, S.A. (2014), "Shear wall effect on material consumption based on seismic design", *Gradevinar*, **66**(1), 1-9.

Amanat, K.M. and Hoque, E. (2006), "A rationale for determining the natural period of RC building frames having infill", *Eng.*

- Struct.*, **28**(4), 495-502.
- Asteris, P.A., Repapis, C.C., Cavaleri, L., Sarhosis, V. and Athanasopoulou, A. (2015), "On the fundamental period of infilled RC frame buildings", *Struct. Eng. Mech.*, **54**(6), 1175-1200.
- Asteris, P.A., Repapis, C.C., Foskolos, F., Fotos, A. and Tsaris, A.K. (2017), "Fundamental period of infilled RC frame structures with vertical irregularity", *Struct. Eng. Mech.*, **61**(5), 663-674.
- Asteris, P.G., Tsaris, A.K., Cavaleri, L., Repapis, C.C., Papalou, A., Di Trapani, F. and Karypidis, D.F. (2016), "Prediction of the Fundamental Period of Infilled RC Frame Structures Using Artificial Neural Networks", *Comput. Intell. Neurosci.*, Volume 2016, Article ID 5104907, 1-12.
- ATC (1978), Tentative provisions for the development of seismic regulations for buildings, Report No. ATC3-06, Applied Technology Council, Palo Alto, California.
- Chandwani, V., Agrawal, V. and Nagar, R. (2015), "Modeling slump of ready mix concrete using genetic algorithms assisted training of artificial neural networks", *Expert Syst. Appl.*, **42**(2), 885-893.
- Cole, E.E., Tokas, C.V. and Meehan, J.F. (1992), "Analysis of recorded building data to verify or improve 1991 Uniform Building Code (UBC) period of vibration formulas", *Proceedings of SMIP92, Strong Motion Instrumentation Program, Divisions of Mines and Geology*, California Department of Conservation, Sacramento.
- Costa Rican Seismic Code (1986), Seismic Code of Costa Rica, Federal College of Engineers and Architects of Costa Rica, San Jose, Costa Rica.
- E.A.K. (2003), Greek Earthquake Resistant Design Code, Earthquake Design and Protection Organization (OASP) and Technical Chamber of Greece (TEE), Athens.
- Egyptian Seismic Code (1988), Regulations for Earthquake Resistant Design of Buildings in Egypt, Egyptian Society for Earthquake Engineering, Cairo, Egypt.
- Ellis, B.R. (1980), "An assessment of the accuracy of predicting the fundamental natural frequencies of building and the implications concerning the dynamic analysis of structures", *Proceedings of the Institution of Civil Engineers*, **69**(2), 763-776.
- EN 1998-1:2004 (2004), Eurocode 8: design of structures for earthquake resistance - part 1: general rules, seismic actions and rules for buildings, European Committee for Standardization.
- FEMA-450 (2003), NEHRP recommended provisions for seismic regulations for new buildings and other structures, Part 1: Provisions, Washington (DC), Federal Emergency Management Agency.
- Gallipoli, M.R., Mucciarelli, M., Šket-Motnikar, B., Zupančič, P., Gosar, A., Prevolnik, S., Herak, M., Stipčević, J., Herak, D., Milutinović, Z. and Olumčeva, T. (2010), "Empirical estimates of dynamic parameters on a large set of European buildings", *Bull. Earthq. Eng.*, **8**, 593-607.
- Gavin, J. and Bowden, G.C. (2005), "Input determination for neural network models in water resources applications. Part 1- background and methodology", *J. Hydrol.*, **301**(1-4), 75-92.
- Gilles, D. (2010), "In situ dynamic properties of buildings in Montreal determined from ambient vibration records", PhD Thesis, Department of Civil Engineering and Applied Mechanics, McGill University Montreal.
- Gilles, D. and McClure, G. (2008), "Development of a period database for buildings in Montreal using ambient vibrations", *Proceedings of the 14th WCEE*, Beijing, China.
- Goel, R.K. and Chopra, A.K. (1998), "Period formulas for concrete shear wall buildings", *J. Struct. Eng.*, **124**(4), 426-433.
- Gonzales, H. and López-Almansa, F. (2012), "Seismic performance of buildings with thin RC bearing walls", *Eng. Struct.*, **34**, 244-258.
- Gutta, S., Philomin, V. and Trajkovic, M. (2005), "Self-organizing feature map with improved performance by non-monotonic variation of the learning rate", Free Patents Online (FPO).
- Hadzima-Nyarko, M., Morić, D., Draganić, H. and Štefić, T. (2015), "Comparison of fundamental periods of reinforced shear wall dominant building models with empirical expressions", *Techn. Gazette*, **22**(3), 685-694.
- Hadzima-Nyarko, M., Nyarko, E.K. and Morić, D. (2011), "A neural network based modelling and sensitivity analysis of damage ratio coefficient", *Expert Syst. Appl.*, **38**(10), 13405-13413.
- Housner, G.W. and Brady, G. (1963), "Natural periods of vibration of buildings", *J. Eng. Mech. Div., Proceedings of the American Society of Civil Engineers*, **89**, No. EM4, 31-65.
- Işik, E. and Kutanis, M. (2015), "Performance based assessment for existing residential buildings in Lake Van basin and seismicity of the region", *Earthq. Struct.*, **9**(4), 893-910.
- Israel IC-413 (1994), SI 413 Design provision for Earthquake Resistant of structures, Standard Institute of Israel 1988.
- Jalali, A. and Salem, A. (2005), "Fundamental periods of buildings measured from ambient vibration measurements", *Proceedings of the 2005 World Sustainable Building Conference*, Tokyo.
- Joshi, S.G., Shreenivas N. Londhe, S.N. and Kwatra, N. (2014), "Application of artificial neural networks for dynamic analysis of building frames", *Comput. Concrete*, **13**(6), 765-780.
- Kalman Šipoš, T., Sigmund, V. and Hadzima-Nyarko, M. (2013), "Earthquake performance of infilled frames using neural networks and experimental database", *Eng. Struct.*, **51**, 113-127.
- KBC (1988), National Building Code of Korea (KBC), Korean Ministry of Construction, Seoul.
- Khademi, F., Akbari, M. and Jamal, S.M.M. (2015), "Prediction of compressive strength of concrete by data-driven models", *i-Manager's J. Civil Eng.*, **5**(2), 16.
- Kohonen, T. (1989), *Self-organization and Associative Memory*, 3rd Edition, Springer, New York.
- Kose, M.M. (2009), "Parameters affecting the fundamental period of RC buildings with infill walls", *Eng. Struct.*, **31**(1), 93-102.
- Kutanis, M., Boru, E.O. and Işik, E. (2016), "Alternative instrumentation schemes for the structural identification of the reinforced concrete field test structure by ambient vibration measurements", *KSCE J. Civil Eng.*, **21**(5), 1793-1801.
- Kwon, O.S. and Kim, E.S. (2010), "Evaluation of building period formulas for seismic design", *Earthq. Eng. Struct. Dyn.*, **39**(14), 1569-1583.
- Lazarevska, M., Knezevic, M., Cvetkovska, M. and Trombeva-Gavriloska, A. (2014), "Application of artificial neural networks in civil engineering", *Tech. Gazette*, **21**(6), 1353-1359.
- Lee, L.H., Chang, K.K. and Chun, Y.S. (2000), "Experimental formula for the fundamental period of RC buildings with shear-wall dominant system", *Struct. Des. Tall Build.*, **9**, 295-307.
- Li, Y. and Mau, S.T. (1997), "Learning from recorded earthquake motion of buildings", *J. Struct. Eng.*, **123**(1), 62-69.
- Massone, L.M. and Ulloa, M.A., (2014), "Shear response estimate for squat reinforced concrete walls via a single panel model", *Earthq. Struct.*, **7**(5), 733-751.
- Michel, C., Guéguen, P., Lestuzzi, P. and Bard, P.Y. (2010), "Comparison between seismic vulnerability models and experimental dynamic properties of existing buildings in France", *Bull. Earthq. Eng.*, **8**, 1295-1307.
- Muhammad, K., Noor Mohammad, N. and Rehman, F. (2015), "Modeling shotcrete mix design using artificial neural network", *Comput. Concrete*, **15**(2), 167-181.
- NeuroSolutions Getting Started Manual Version 4, Neural Network Based System Identification Toolbox (2005), Retrieved from <http://www.neurosolutions.com/>.
- New Zealand Society of Earthquake Engineering (NZSEE) (2006),

- Assessment and improvement of the structural performance of buildings in earthquakes, Recommendations of a NZSEE Study Group on Earthquake Risk Buildings.
- Nikoo, M., Torabian Moghadam, F. and Sadowski, L. (2015), "Prediction of concrete compressive strength by evolutionary artificial neural networks", *Adv. Mater. Sci. Eng.*, Volume 2015, Article ID 849126, 1-8.
- Nikoo, M., Zarfam, P. and Sayahpour, H. (2015), "Determination of compressive strength of concrete using Self Organization Feature Map (SOFM)", *Eng. Comput.*, **31**(1), 113-121.
- NSCP (1992), National Structural Code of Philippines, Vol. 1, Fourth Edition, The Board of Civil Engineering of the Professional Regulation Commission, Manila, Philippines.
- Oliveira, C.S. and Navarro, M. (2010), "Fundamental periods of vibration of RC buildings in Portugal from in-situ experimental and numerical techniques", *Bull. Earthq. Eng.*, **8**(3), 609-642.
- Ozmen, H.B. and Inel, M. (2015), "Damage potential of earthquake records for RC building stock", *Earthq. Struct.*, **10**(6), 1315-1330.
- Poovarodom, N., Warnitchai, P., Petcharoen, C., Yinghan, P. and Jantasod, M. (2004), "Dynamic characteristics of non-seismically designed reinforced concrete buildings with soft soil condition in Bangkok", *Proceedings of the 13th WCEE*, Vancouver, B.C., Canada, Paper No. 1264.
- Ricci, P., Verderame, G.M. and Manfredi, G. (2011), "Analytical investigation of elastic period of infilled RC MRF buildings", *Eng. Struct.*, **33**, 308-319.
- Sadowski, L. and Hola, J. (2015), "ANN modeling of pull-off adhesion of concrete layers", *Adv. Eng. Softw.*, **89**, 17-27.
- Salama, M.I. (2015), "Estimation of period of vibration for concrete moment-resisting frame buildings", *HBRC J.*, **11**, 16-21.
- SEAOC (1996), Recommended lateral force requirements and commentary, Seismological Engineers Association of California, San Francisco.
- Sofi, M., Hutchinson, G.L. and Duffield, C. (2015), "Review of techniques for predicting the fundamental period of multi-storey buildings: effects of nonstructural components", *Int. J. Struct. Stab. Dyn.*, **15**(02), 1450039.
- Tay, F.E.H. and Cao, L.J. (2001), "Improved financial time series forecasting by combining support vector machines with self-organizing feature map", *Intell. Data Anal.*, **5**(4), 339-354.
- UBC-Uniform Building Code (1997), International conference of building officials. Whittier, CA.
- Yuan, Z., Wang, L.N. and Ji, X. (2014), "Prediction of concrete compressive strength: Research on hybrid models genetic based algorithms and ANFIS", *Adv. Eng. Softw.*, **67**, 156-163.
- Zhou, Y., Zhou, Y., Yi, W., Chen, T., Tan, D. and Mi, S. (2017), "Operational modal analysis and rational finite-element model selection for ten high-rise buildings based on on-site ambient vibration measurements", *J. Perform. Constr. Facil.*, **31**(5), 1-14.